Figures and figure supplements

A generic binding pocket for small molecule I_{Ks} activators at the extracellular inter-subunit interface of KCNQ1 and KCNE1 channel complexes

Magnus Chan, Harutyun Sahakyan and Jodene Eldstrom *et al*.

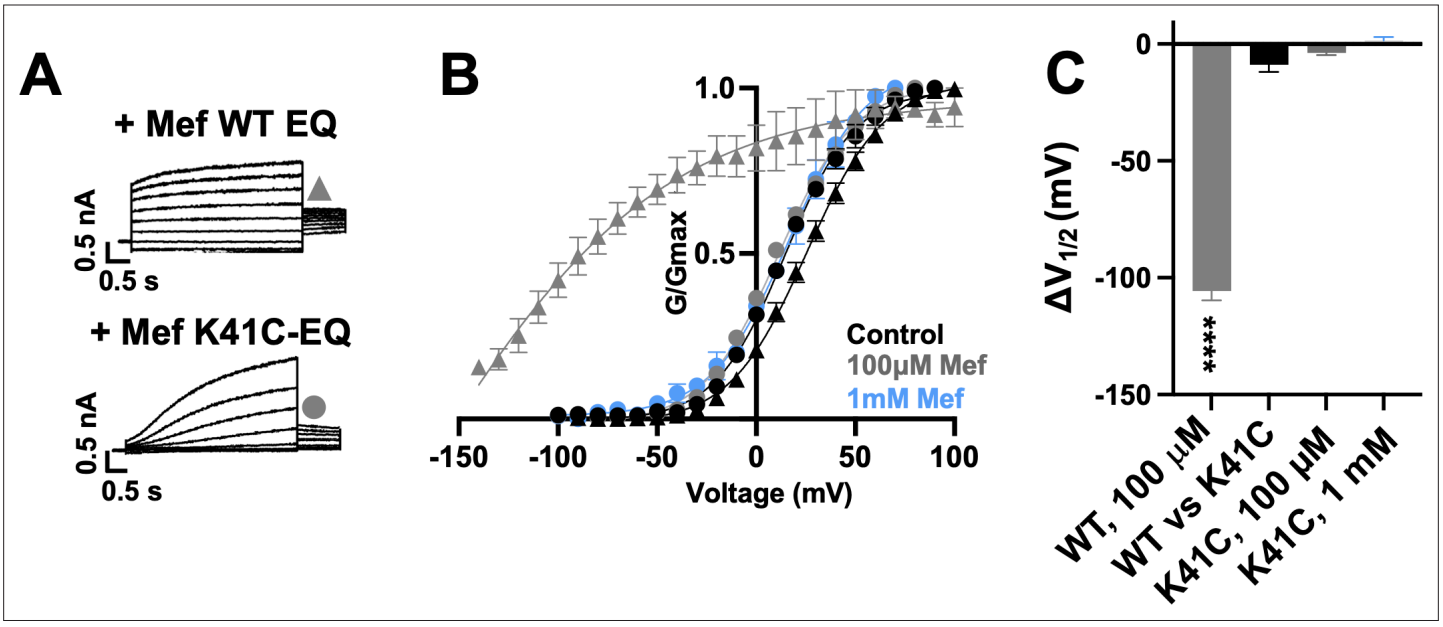

Figure 1. K41C-KCNE1 mutants prevent the agonist effect of mefenamic acid. (**A**) Current traces of WT EQ (top) and K41C-EQ (bottom) in the presence of 100 μM mefenamic acid (Mef). A 4 s protocol was used with pulses from –150 mV or higher to +100 mV, in 10 mV steps, followed by a repolarization step to –40 mV for 1 s. Holding potential and interpulse interval were –80 mV and 15 s, respectively. (**B**) G-V plots obtained from WT EQ tail currents (triangles) and K41C-EQ (circles) in the absence (control: black) and presence of Mef (100 μM: grey; 1 mM: light blue). Boltzmann fits were: WT EQ control (n=6): $V_{1/2}$ = 25.4 mV, *k*=19.4 mV; WT EQ 100 μM Mef (n=3): $V_{1/2}$ = -80.3 mV, *k*=41.3 mV; K41C-EQ control (n=4): $V_{1/2}$ = 15.2 mV, *k*=18.4 mV; K41C-EQ 100 μM Mef (n=4): $V_{1/2}$ = 11.4 mV, *k*=19.4 mV; and K41C-EQ 1 mM Mef (n=3): $V_{1/2}$ = 16.7 mV, *k*=19.8 mV. Error bars shown are SEM. (**C**) Summary plot of $V_{1/2}$ change ($\Delta V_{1/2}$) for WT EQ in the presence of 100 μM mefenamic acid, WT EQ vs K41C-EQ in control and K41C-EQ in the presence of 100 μM and 1 mM mefenamic acid. Data are shown as mean ± SEM and unpaired t-test was used. **** denotes a significant $\Delta V_{1/2}$ compared to control where p<0.0001.

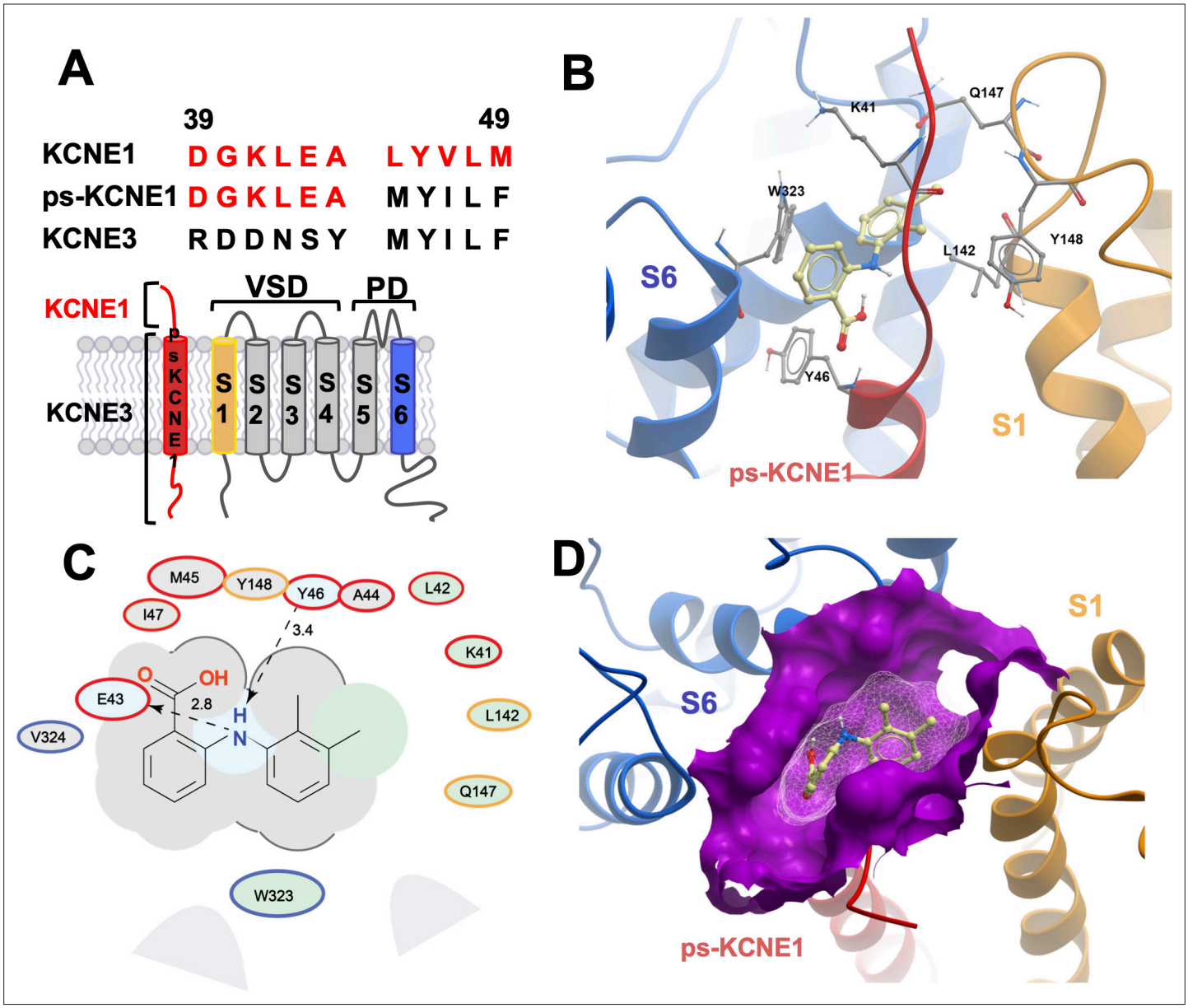

Figure 2. MD prediction of mefenamic acid binding site in the ps-I_{Ks} model. (**A**) Pseudo-KCNE1 (ps-KCNE1) used to predict Mef binding site. Extracellular residues of KCNE1 (top), ps-KCNE1 (middle) and KCNE3 (bottom). Below, cartoon topology of the single transmembrane ps-KCNE1 β-subunit and the six transmembrane KCNQ1 α-subunit. S1-S4 transmembrane segments form the voltage sensor domain and S5-S6 form the pore domain. (**B**) Binding pose of Mef (yellow) in the external region of the ps-I_{Ks} channel complex obtained with docking (side view). Pore domain residues are blue, ps-KCNE1 subunit red, and the VSD of a neighbouring subunit is in yellow. (**C**) Ligand interaction map of Mef with ps-I_{Ks} from molecular docking. Size of residue ellipse is proportional to the strength of the contact. The distance between the residue label and ligand represents proximity. Grey parabolas represent accessible surface for large areas. Light grey ellipses indicate residues in van der Waals contacts, light green ellipses are hydrophobic contacts, and light blue are H-bond acceptors. Red borders indicate KCNE1, yellow are KCNQ1 VSD, and blue are pore residues. Dashed lines indicate H-bonds. The 2D diagram was generated by ICM pro software with cut-off values for hydrophobic contacts of 4.5 Å and hydrogen bond strength of 0.8. Further details in Materials and methods. (**D**) Mef binding pose observed in MD simulations in space-fill to highlight pocket formed by external S1 (yellow), S6 (blue) transmembrane domains of KCNQ1, and extracellular region of the ps-KCNE1 subunit (red). This binding conformation is the most frequent binding pose of Mef observed in ~50% of frames and corresponds to the blue-framed conformation in ***Figure 2—figure supplement 3***.

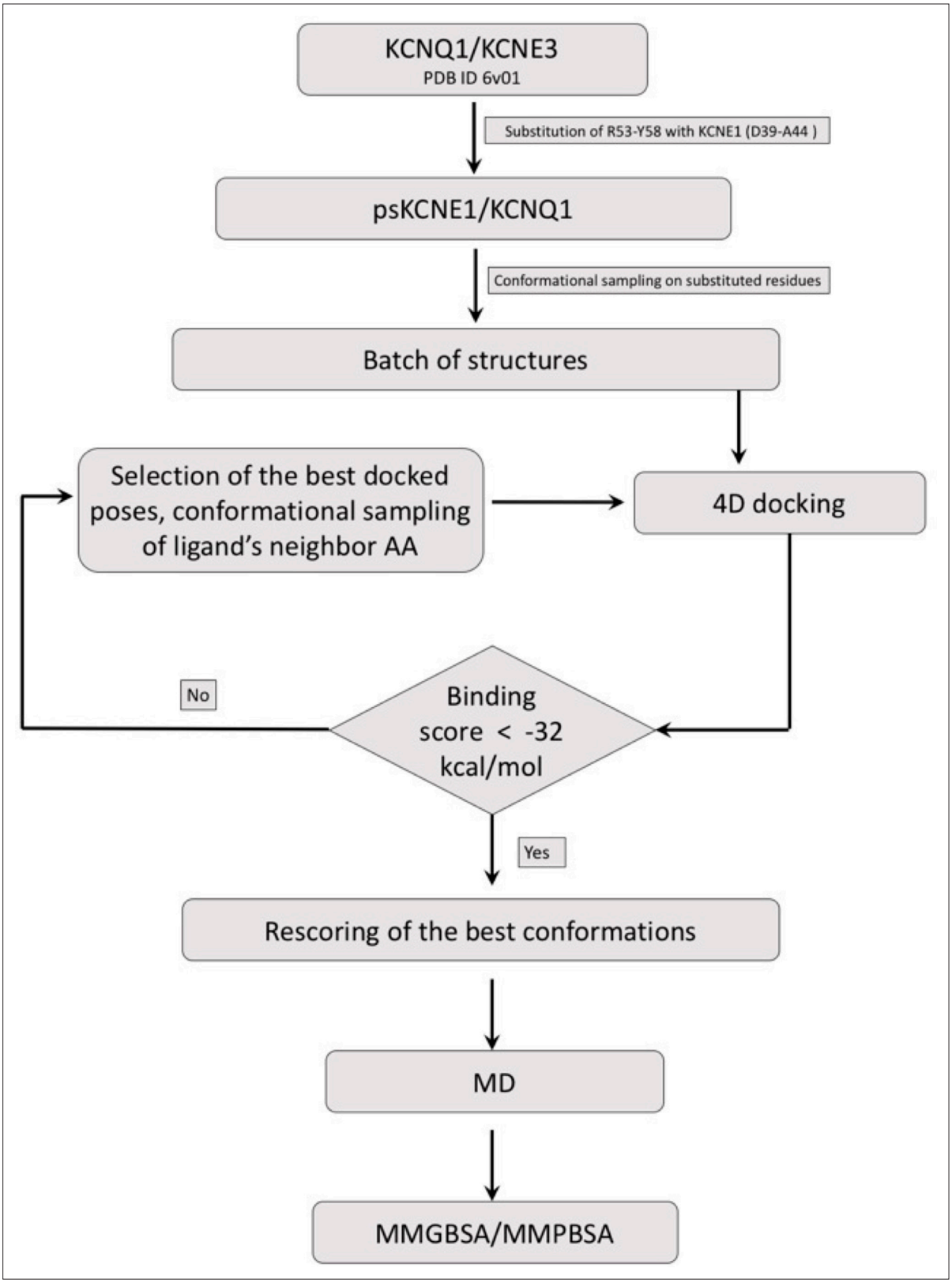

Figure 2—figure supplement 1. Drug docking and MD simulation workflow. Schematic representation of the general workflow for construction of ps-I_{Ks}, Mef docking to the model ps-I_{Ks} channel complex, and MD simulations (See Materials and methods).

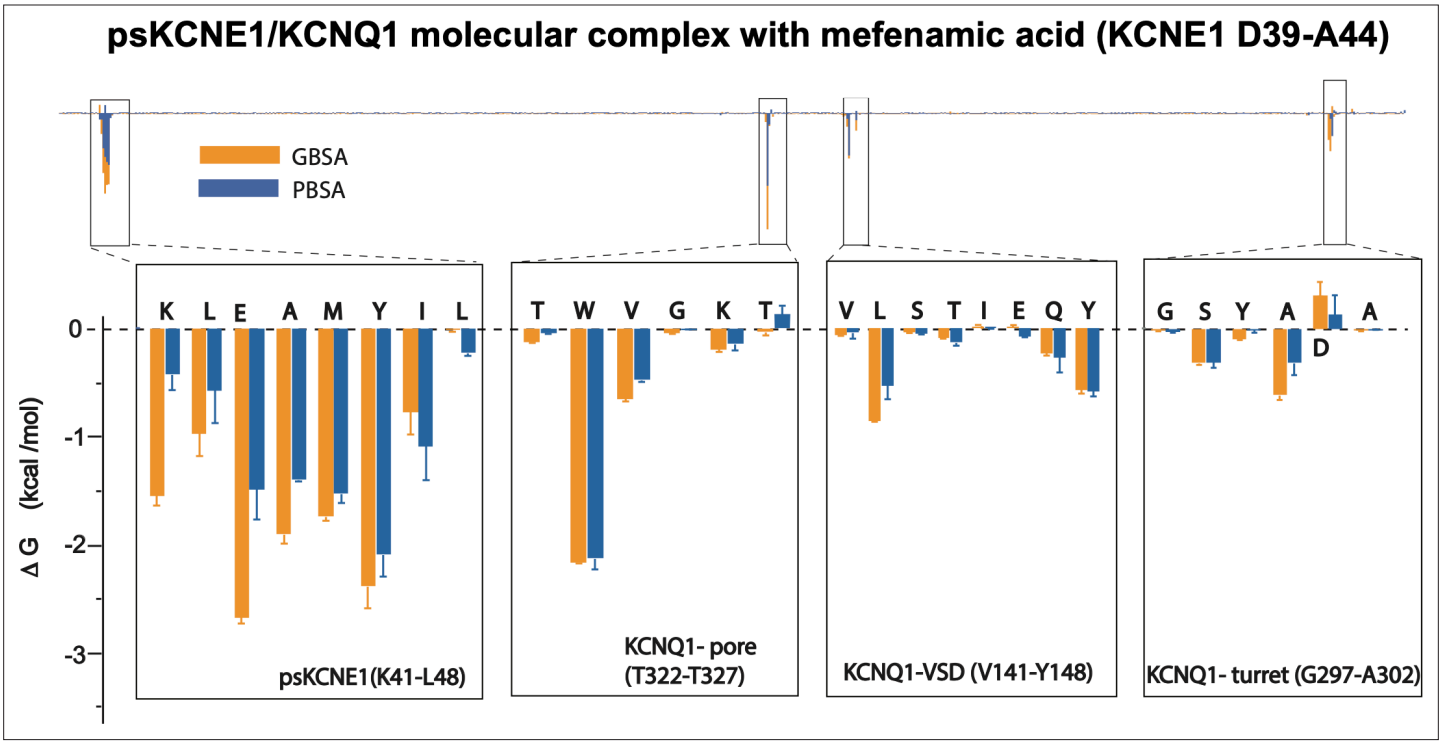

Figure 2—figure supplement 2. Energy decomposition per amino acid for mefenamic acid binding to ps-I_{Ks}. Poisson-Boltzmann Surface Area (MM/PBSA; blue) and Generalized Born Surface Area (MM/GBSA; orange) methods were used to estimate the interaction free energy contribution of each residue in the Mef-bound ps-I_{Ks} complex. Free energy for residues located in ps-KCNE1, pore domain and voltage-sensor domain of KCNQ1, that stand above background, are shown as enlarged panels. Error bars represent ± SD. 1000 frames for each simulation (n=3) were analyzed.

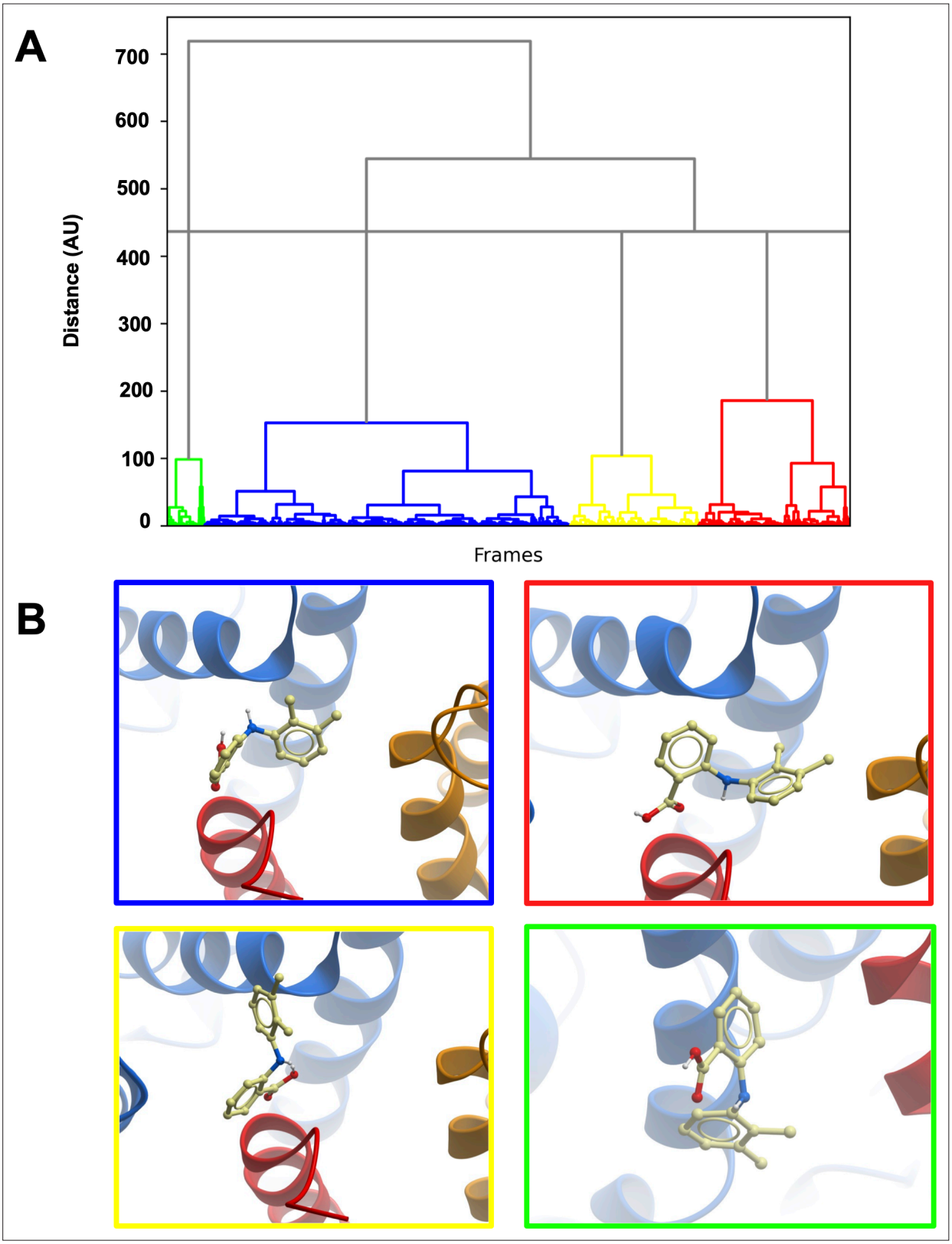

Figure 2—figure supplement 3. Clustering of MD trajectories based on mefenamic acid conformations. (**A**) The clustering dendrogram based on Mef RMSD illustrates the similarity of Mef conformations in MD trajectories. (**B**) Centroids from each cluster with the lowest RMSD compared to all other conformations in the cluster. The color frame around the panels shows to which cluster the depicted conformation belongs.

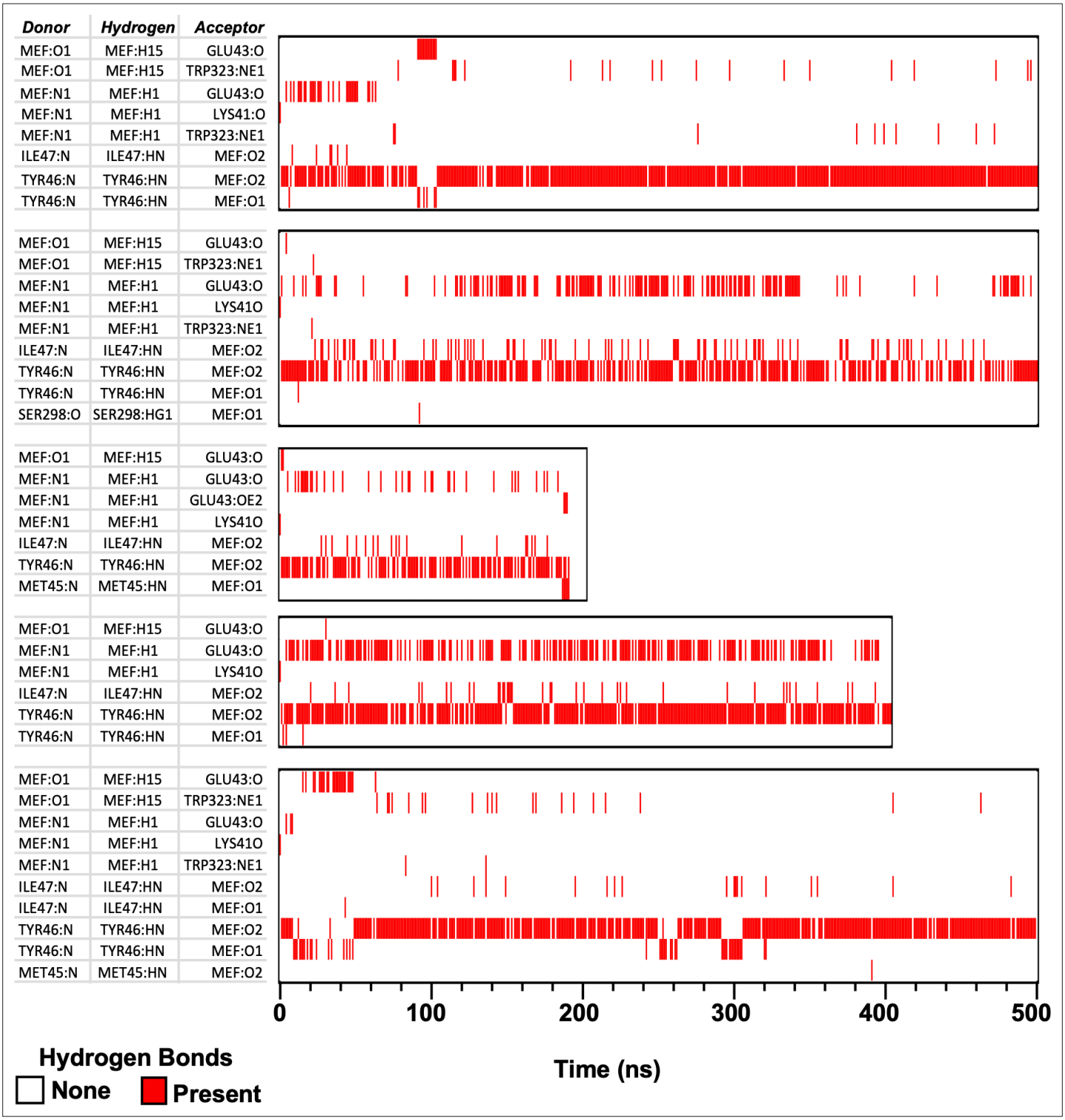

Figure 2—figure supplement 4. H-bonds formed between mefenamic acid and protein residues in its binding site during MD simulations. MEF-N1 indicates the nitrogen of aminobenzoic acid; MEF:O1 and O2 are the oxygens of the aminobenzoic acid. Red lines indicate at which time point and between which atoms H-bond were formed.

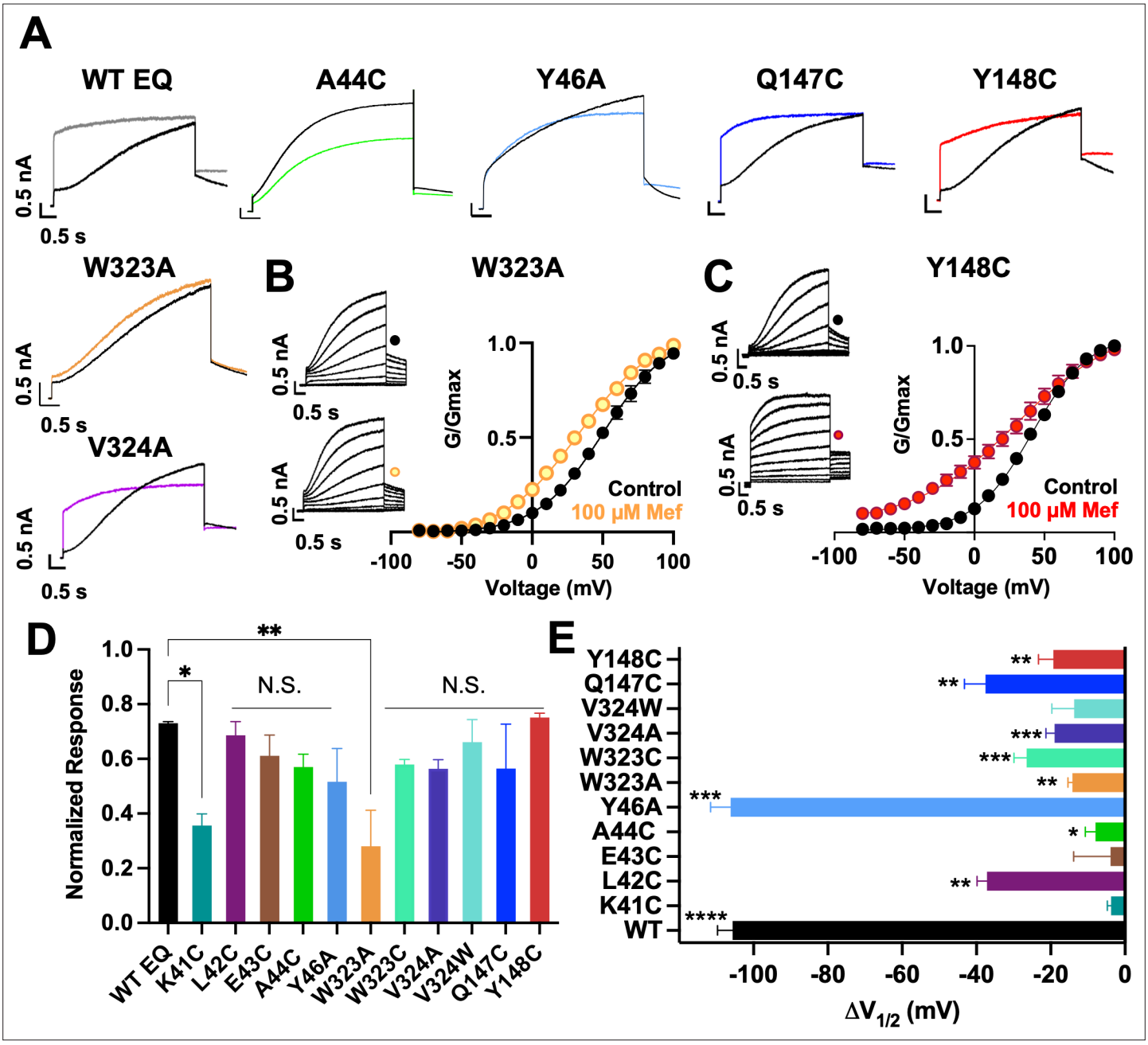

Figure 3. Current waveform and G-V changes induced by mefenamic acid in binding site mutants. (**A**) Current traces from WT EQ and key residue mutants in control (black) and 100 µM Mef (colors). (**B**) EQ-W323A and (**C**) EQ-Y148C current traces in control (top) and presence of 100 µM Mef (below). G-V plots in control (black) and presence of 100 µM Mef (colors). Boltzmann fits were: EQ-W323A control (n=4): $V_{1/2}$ = 47.8 mV, *k*=23.7 mV; EQ-W323A Mef (n=3): $V_{1/2}$ = 33.7 mV, *k*=28.5 mV; EQ-Y148C control (n=4): $V_{1/2}$ = 36.8 mV, *k*=20.3 mV; and EQ-Y148C Mef (n=4): $V_{1/2}$ = 17.5 mV, *k*=36.7 mV. Voltage steps were from –80 mV to +100 mV for 4 s, followed by a 1 s repolarization to –40 mV. Interpulse interval was 15 s. Error bars shown are ± SEM. (**D**) Summary plot of the normalized response to 100 µM Mef (see Materials and methods). Data are shown as mean + SEM and one-way ANOVA statistical test was used. **p<0.01 and *p<0.05 denote a significantly reduced response compared to WT EQ. N.S. denotes not significant. (**E**) Change in $V_{1/2}$ ($\Delta V_{1/2}$) for WT EQ and each I_{Ks} mutant in control versus mefenamic acid. Data are shown as mean -SEM and unpaired t-test was used, where *p<0.05, **p<0.01, ***p<0.001, ****p<0.0001 indicate a significant change in $V_{1/2}$ comparing control to the presence of the drug. n-values for mutants in D and E are stated in ***Table 1***.

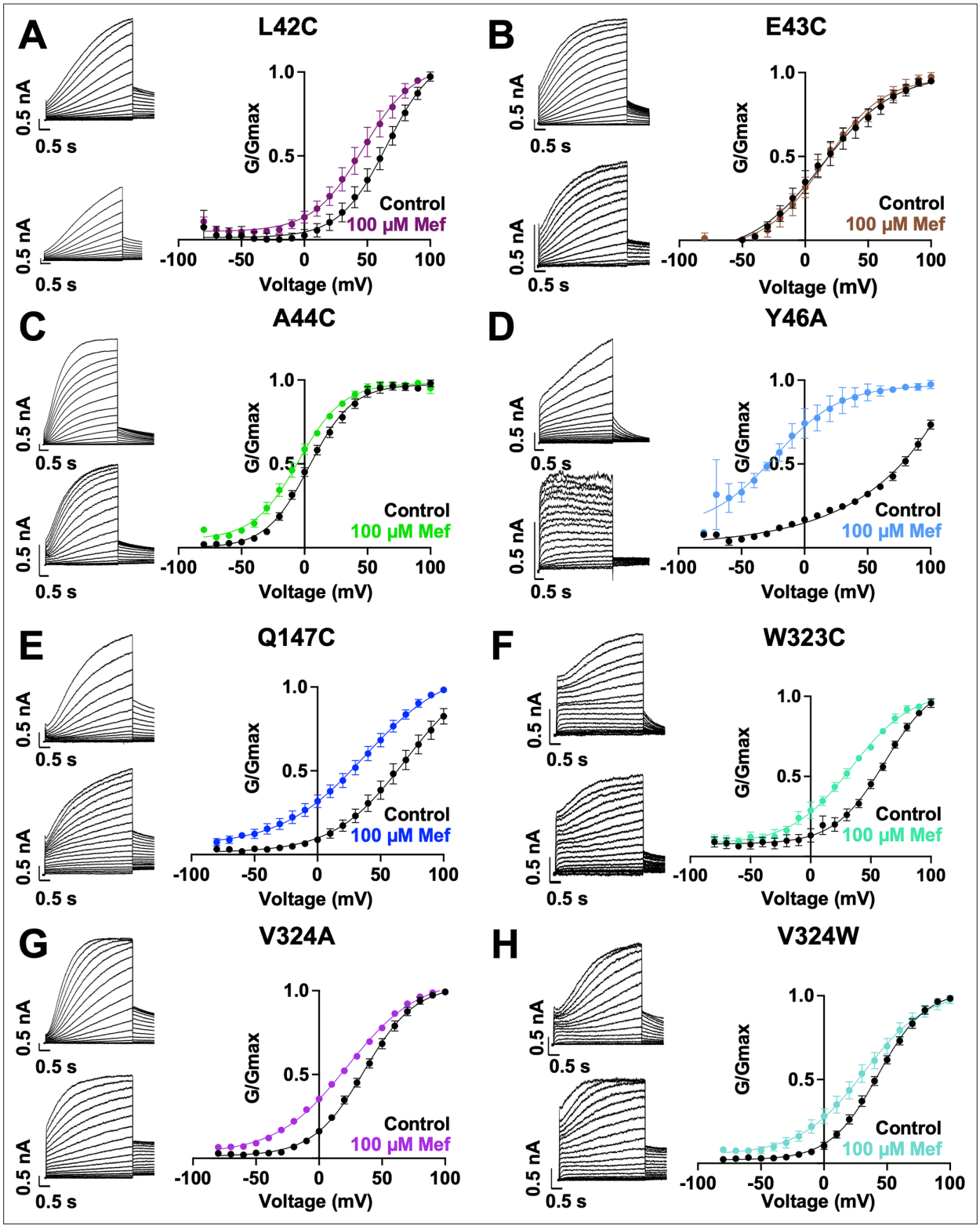

Figure 3—figure supplement 1. Current waveform and G-V changes induced by mefenamic acid for all binding site mutants. (**A**)-(**H**) current traces in control (above) and presence of 100 µM Mef (below) and G-V plots for binding site mutants, as indicated. Cells were held at –80 mV, then pulsed from –90 mV to +100 mV for 4 s followed by –40 mV for 2 s. Error bars shown are ± SEM. Refer to ***Table 1*** for Boltzmann fit values.

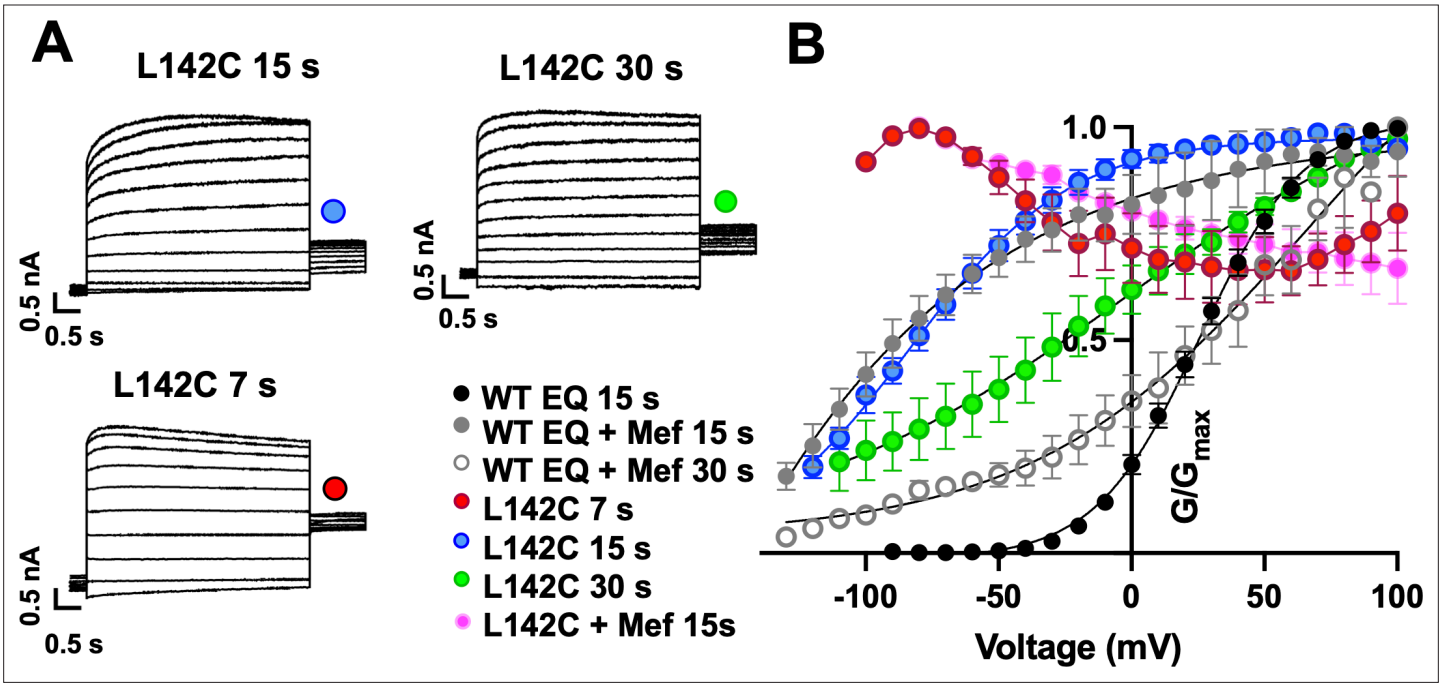

Figure 3—figure supplement 2. Augmented activation of EQ-L142C in the absence of mefenamic acid. (**A**) EQ-L142C current traces in control solutions. Voltage steps were from –130 mV or higher in 10 mV steps to +100 mV for 4 s, followed by a repolarization step to –40 mV for 1 s. Holding potential was –80 mV. Interpulse interval was as indicated above, 15 s, 30 s and 7 s. (**B**) G-V plot of WT EQ in control (interpulse interval 15 s: black) and in the presence of 100 μM Mef (interpulse interval 15 s: grey closed circle; 30 s: grey open circle) and EQ-L142C in control solutions (interpulse interval 7 s: red; 15 s: blue; 30 s: green). Boltzmann fits were: WT EQ 15 s control (n=6): $V_{1/2}$ = 25.4 mV, *k*=19.4 mV; WT EQ 15 s Mef (n=3): $V_{1/2}$ = -80.3 mV, *k*=41.3 mV; WT EQ 30 s Mef (n=8); $V_{1/2}$ = 26.7 mV, *k*=66.6 mV; EQ-L142C 15 s control (n=6) $V_{1/2}$ = -80.3 mV, *k*=30.0 mV; EQ-L142C 30 s control (n=3) $V_{1/2}$ = -28.7 mV, *k*=62.5. Due to the dramatic change in G-V plot shape, Boltzmann fits were not possible for EQ-L142C with an interpulse interval of 7 s. All mutations are forced saturated I_{Ks} channel complexes. Error bars shown are ± SEM.

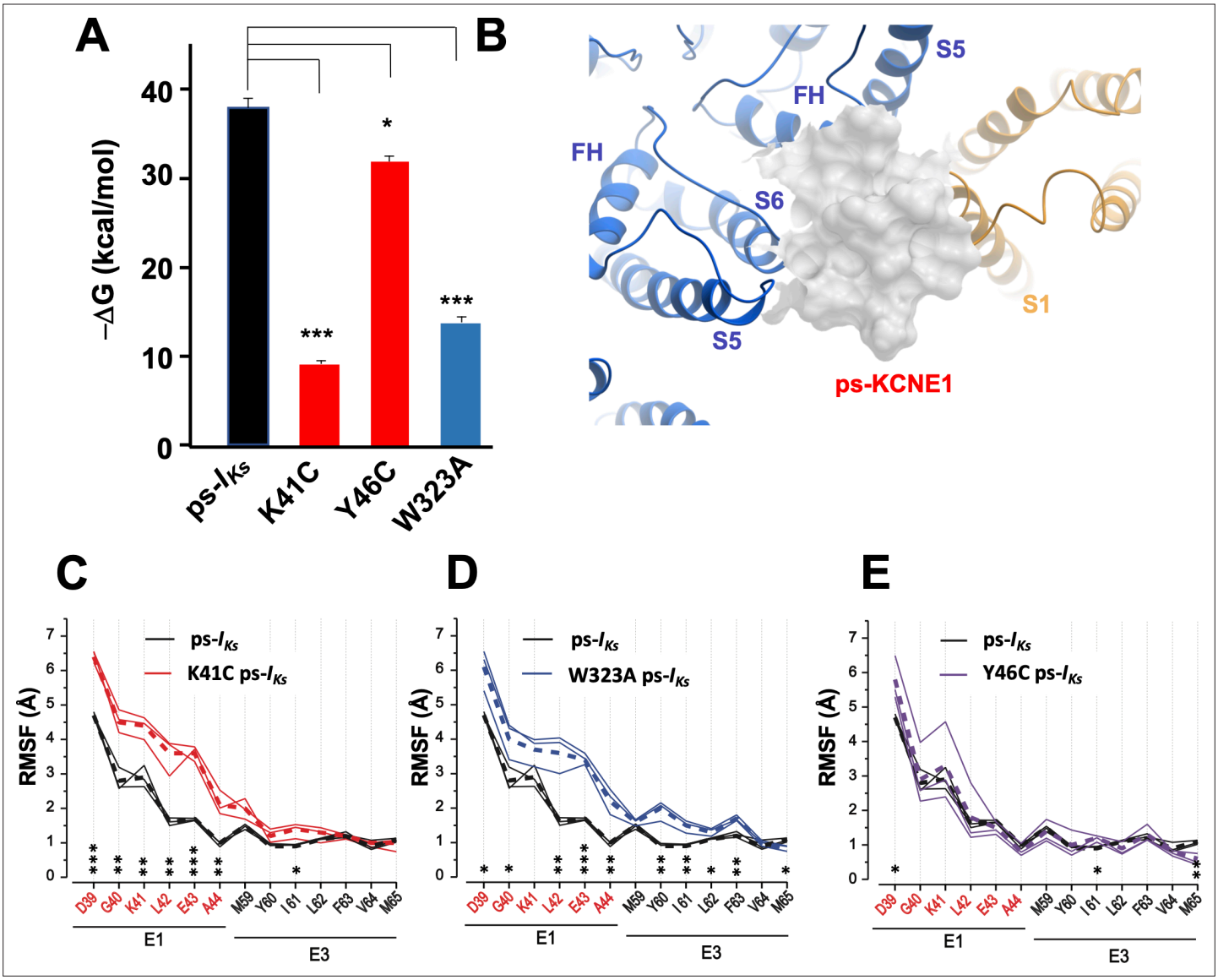

Figure 4. K41C, Y46C, and W323A mutant impact on mefenamic acid binding energy and flexibility of external KCNE1 residues. (**A**) Average free interaction energy of Mef-bound ps-I_{Ks} complexes calculated using MM/GBSA methods from three independent MD simulation runs. For K41C and W323A mutations, calculations correspond to interval of simulations before the detachment of ligand from the molecular complex. * and *** denote significant differences in average free interaction energy compared to ps-I_{Ks}. Student`s unpaired t-test was used for comparison of groups. (**B**) Surface representation of ps-I_{Ks} after removal of Mef. The pore residues are in blue and the VSD of a neighbouring subunit is yellow. (**C–E**) Root mean square fluctuations (RMSF) of ps-KCNE residues (Å) in the ps-I_{Ks} complex during the last 100 ns of simulations. Three separate MD simulations shown for the ps-I_{Ks} channel without Mef (black lines) and three for K41C (C, red), W323A (D, blue) after ligand detachment, and Y46C in absence of ligand (E, purple). Dashed lines show average values of RMSF calculated from three simulations. ***p<0.001; **p<0.01 *p<0.05 using an unpaired t-test. GROMACS software was used for RMSF analysis.

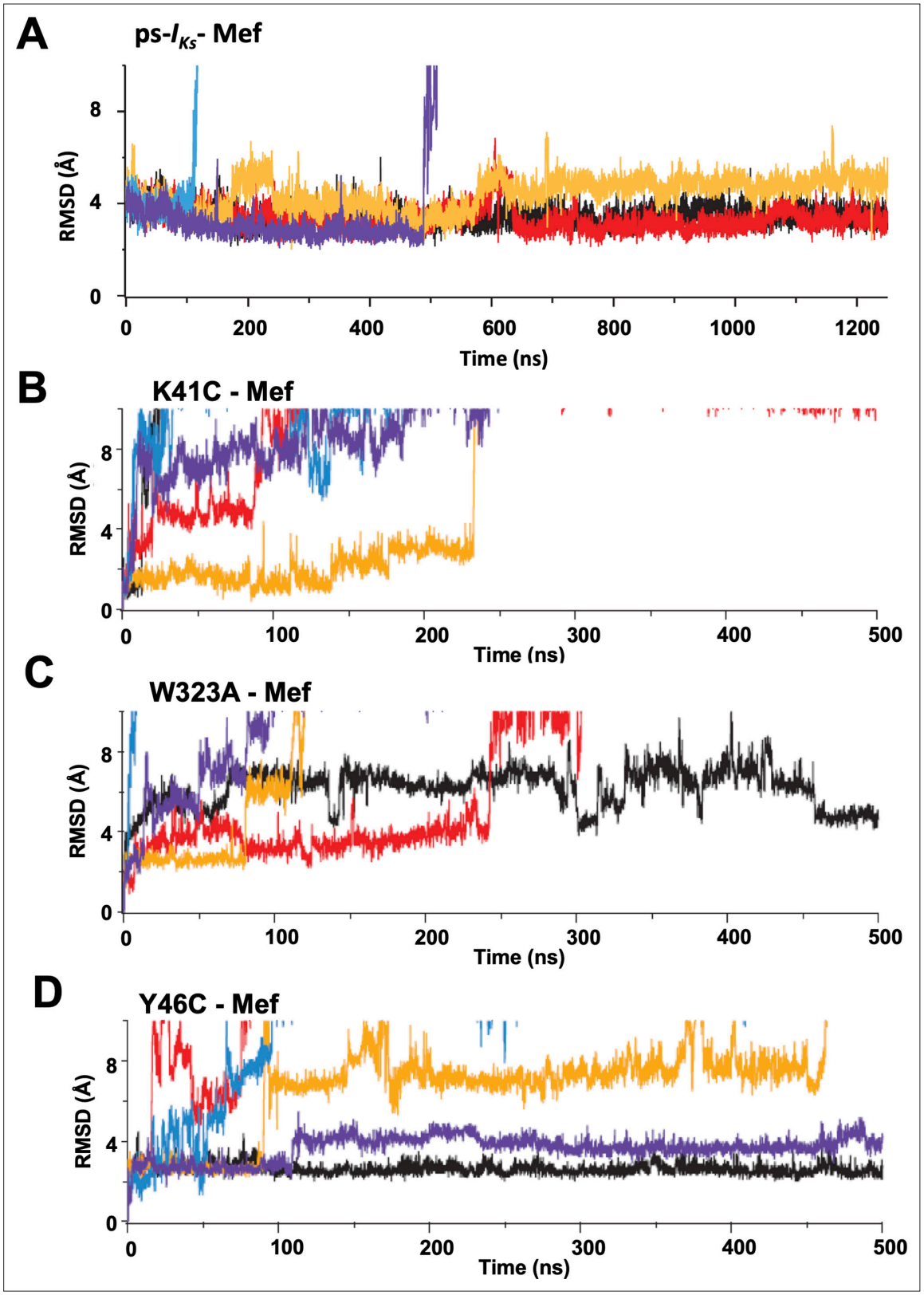

Figure 4—figure supplement 1. Root-mean-square deviations (RMSD) of mefenamic acid from its initial position during MD simulations. (**A**) ps-I_{Ks}, (**B**) K41C, (**C**) W323A, and (**D**) Y46C-I_{Ks} mutants in the presence of mefenamic acid. Each color represents an individual simulation run, five in each case. Note that time scale in (**A**) is 2.5 x extended compared with (**B–D**).

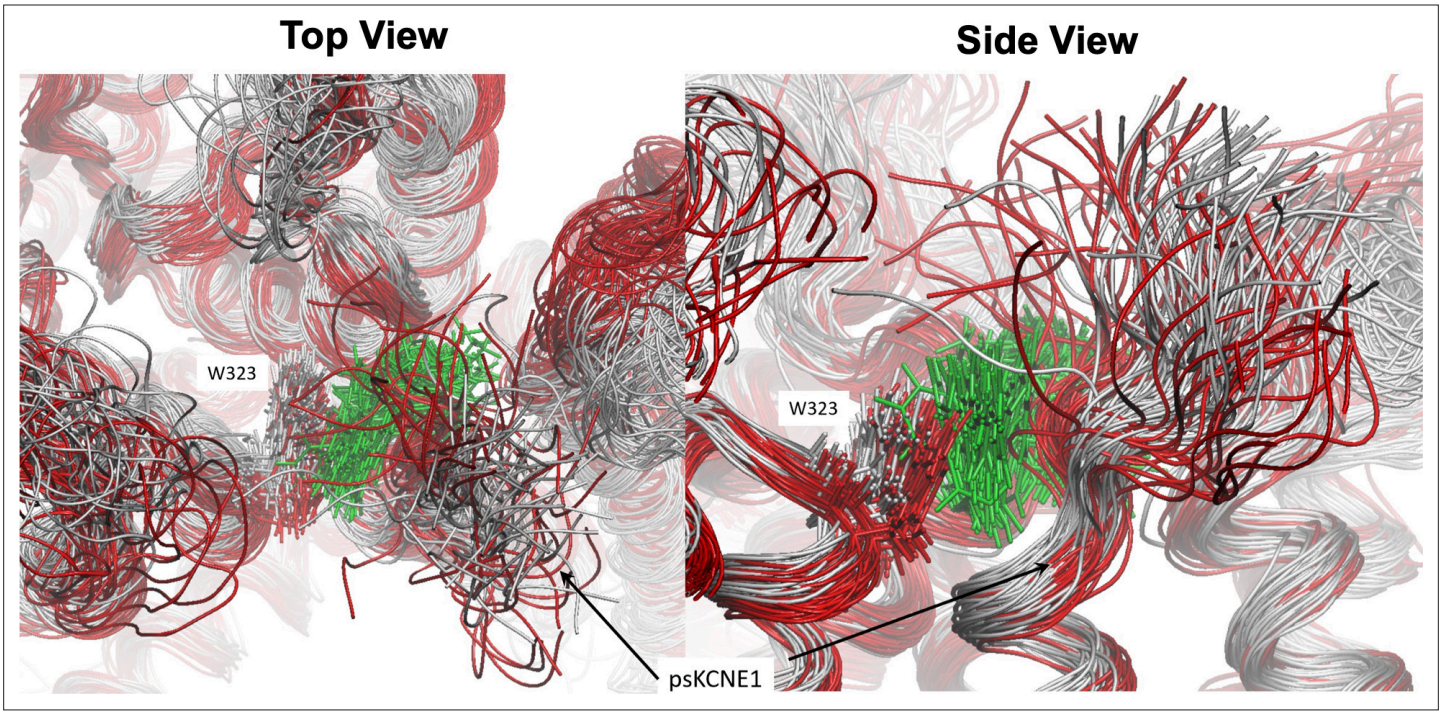

Figure 4—figure supplement 2. Result of loss of mefenamic acid from the binding site. The binding pocket viewed from above (left) and the side (right) during a 1250 ns MD simulation before drug detachment (grey superimposed structure) and after (red superimposed structure). Mefenamic acid is represented as licorice and colored green. Snapshots for superimposition were collected every 10 ns. Visible from the snapshots is that when the drug leaves the binding site (after 500 ns, structures colored red), the N-terminal residues of ps-KCNE1, as well as W323 and other residues that form the pocket, shift toward the space that mefenamic acid previously occupied.

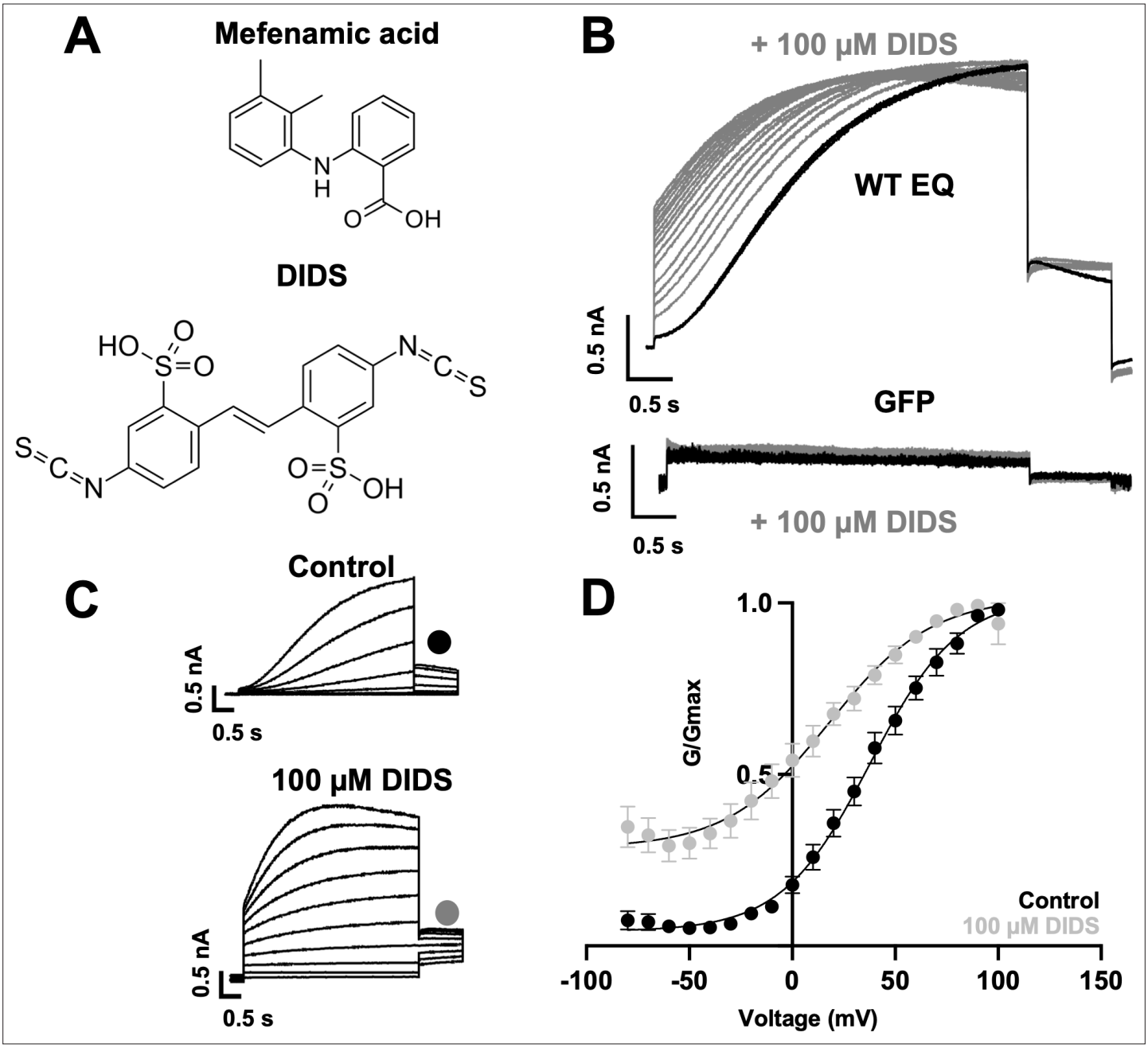

Figure 5. Effect of DIDS on I_{Ks}. (**A**) Molecular structure of mefenamic acid and DIDS. (**B**) WT EQ current in control (black) and exposed to 100 µM DIDS over time (grey). Pulses were from –80 to +60 mV every 15 s, and current traces are shown superimposed. Lower panel shows no effect on currents from GFP-only transfected cells exposed to 100 µM DIDS over time (grey). (**C**) Current traces from WT EQ in control and presence of 100 µM DIDS as indicated. Pulses were from –80 to +100 mV for 4 s, with a 1 s repolarization to –40 mV. Interpulse interval was 15 s. (**D**) Corresponding G-V plot in control (black) and DIDS (grey) from data as shown in panel C. Boltzmann fits were: WT EQ control (n=8): $V_{1/2}$ = 30.5 mV, *k*=20.3 mV; WT EQ in the presence of DIDS (n=5): $V_{1/2}$ = -16.1 mV, *k*=25.3 mV. Error bars shown are ± SEM.

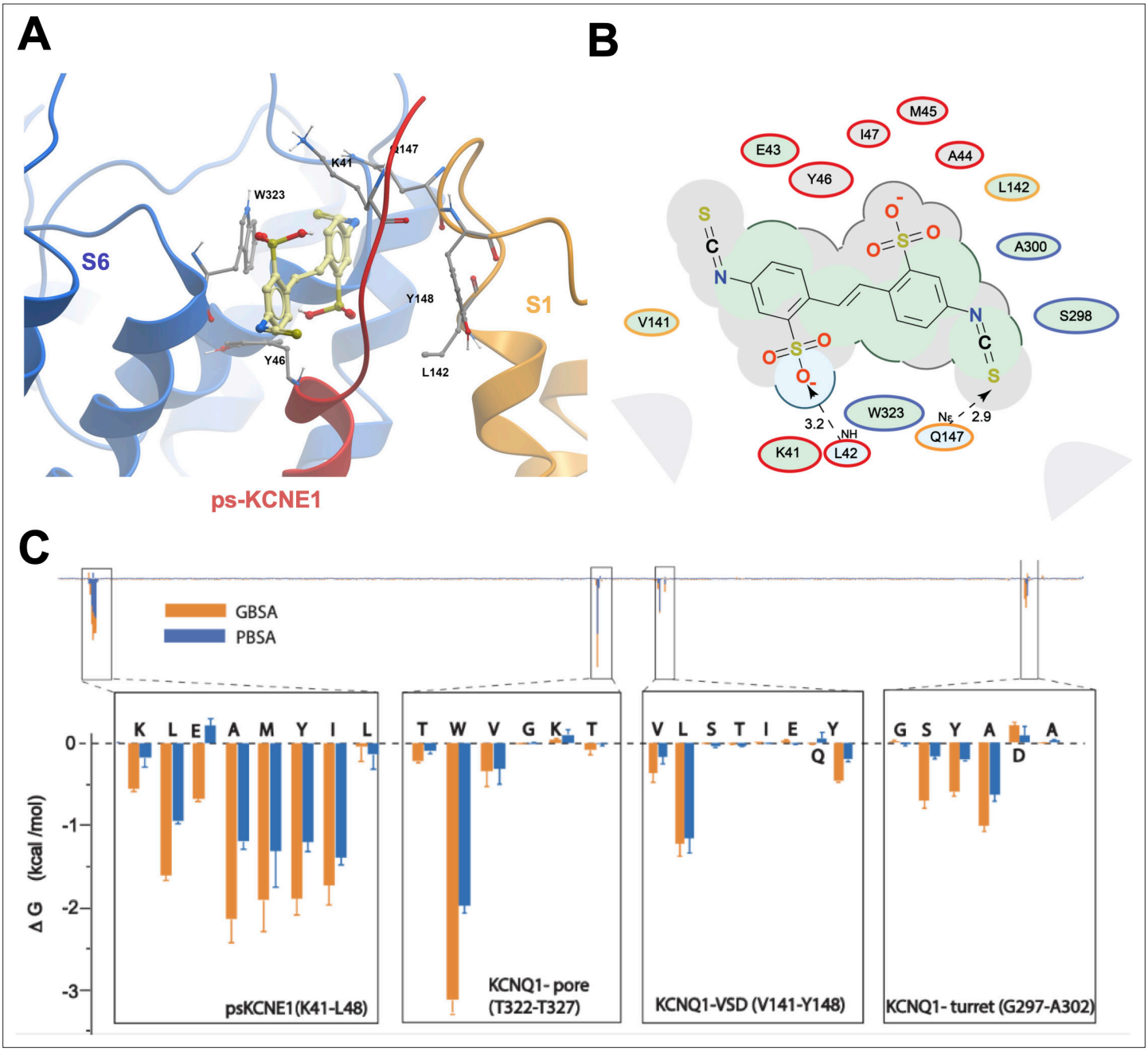

Figure 6. Ligand interaction and energy decomposition per amino acid for DIDS binding to ps-I_{Ks}. (**A**) Binding pose of DIDS (yellow) in the external region of the ps-I_{Ks} channel complex obtained with molecular docking (side view). The residues of the pore domain are colored in blue, ps-KCNE1 subunit in red, and the voltage-sensor domain of a neighbouring subunit is presented in yellow. (**B**) Ligand interaction map of DIDS with ps-I_{Ks} from molecular docking. Size of residue ellipse is proportional to the strength of the contact. Light grey indicates residues in van der Waals contacts, light green hydrophobic contacts, and light blue are hydrogen bond acceptors. Red borders indicate KCNE1 residues, yellow are KCNQ1 VSD residues, and blue are pore residues. Dashed lines indicate H-bonds. The distance between the residue label and ligand represents proximity. Grey parabolas represent accessible surface for large areas. The 2D diagram was generated by ICM pro software with a cut-off value for hydrophobic contacts 4.5 Å and hydrogen bond strength 0.8. (**C**) Energy decomposition per amino acid for DIDS binding to ps-I_{Ks}. Generalized Born Surface Area (MM/GBSA; orange) and Poisson-Boltzmann Surface Area (MM/PBSA; blue) methods were used to estimate the interaction free energy contribution of each residue in the DIDS-bound ps-I_{Ks} complex. The lowest interaction free energy for residues in ps-KCNE1 and selected KCNQ1 domains are shown as enlarged panels (n=3 for each point). Error bars indicate ± SD.

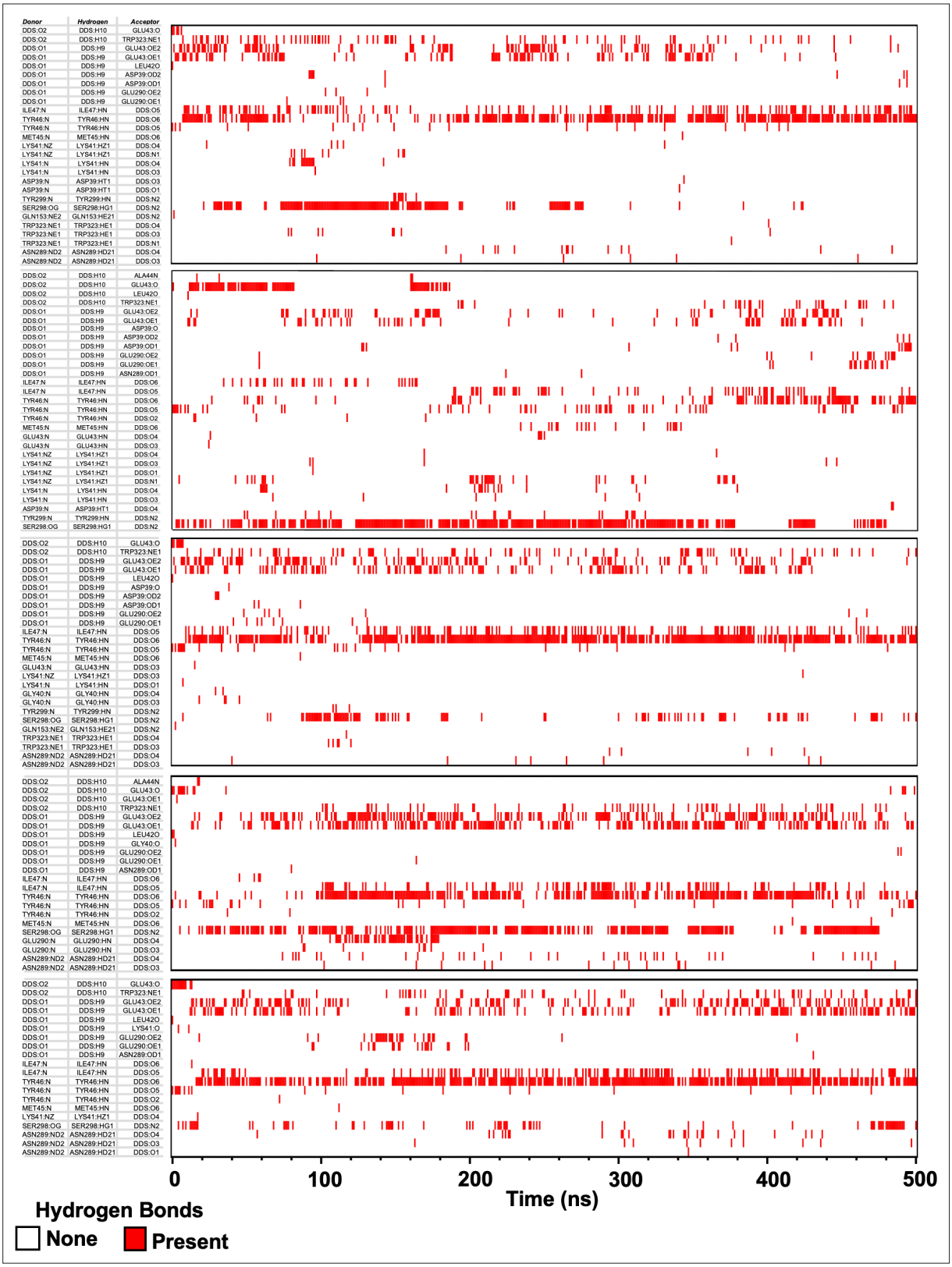

Figure 6—figure supplement 1. H-bonds formed between DIDS and protein residues in its binding site during MD simulations. DDS:O1-O6 are the oxygens of the sulfonic acids; DDS:N1 and N2 are nitrogens of the isothiocyanates. Red lines indicate at which time point and between which atom H-bonds were formed.

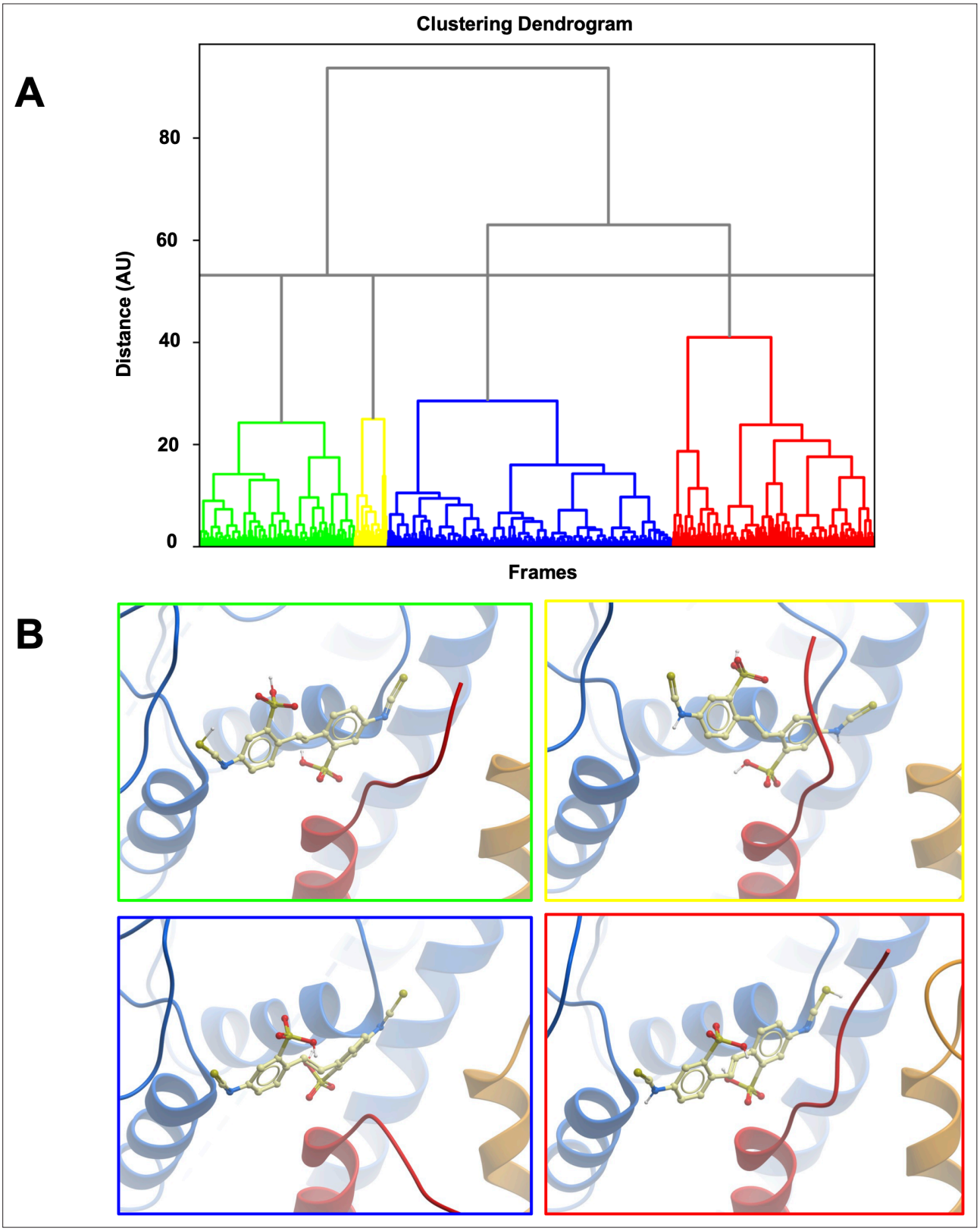

Figure 6—figure supplement 2. Clustering of MD trajectories based on DIDS conformations. (**A**) The clustering dendrogram based on RMSD illustrates the similarity of DIDS conformations in MD trajectories. (**B**) Centroids from each cluster with the lowest RMSD compared to all other conformations in the cluster were selected and overlayed for comparison. The color of the frame around the panel shows to which cluster the depicted conformation belongs.

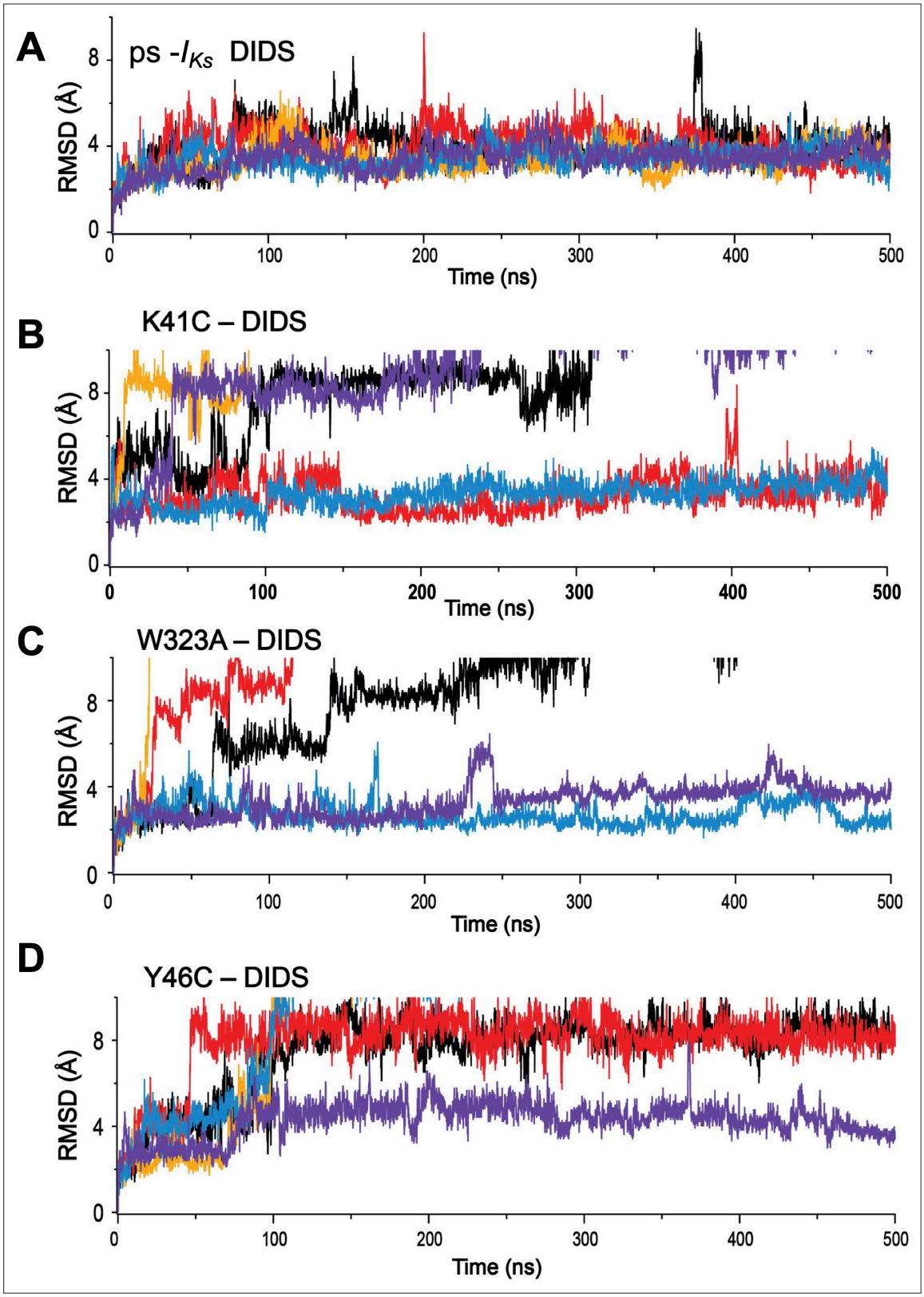

Figure 6—figure supplement 3. Root-mean-square deviations (RMSD) of DIDS from its initial position during MD simulations. (**A**) ps-I_{Ks}, and mutations, (**B**) K41C, (**C**) W323A, and (**D**) Y46C complexes. Individual runs are shown in separate colors, n=5 for each.

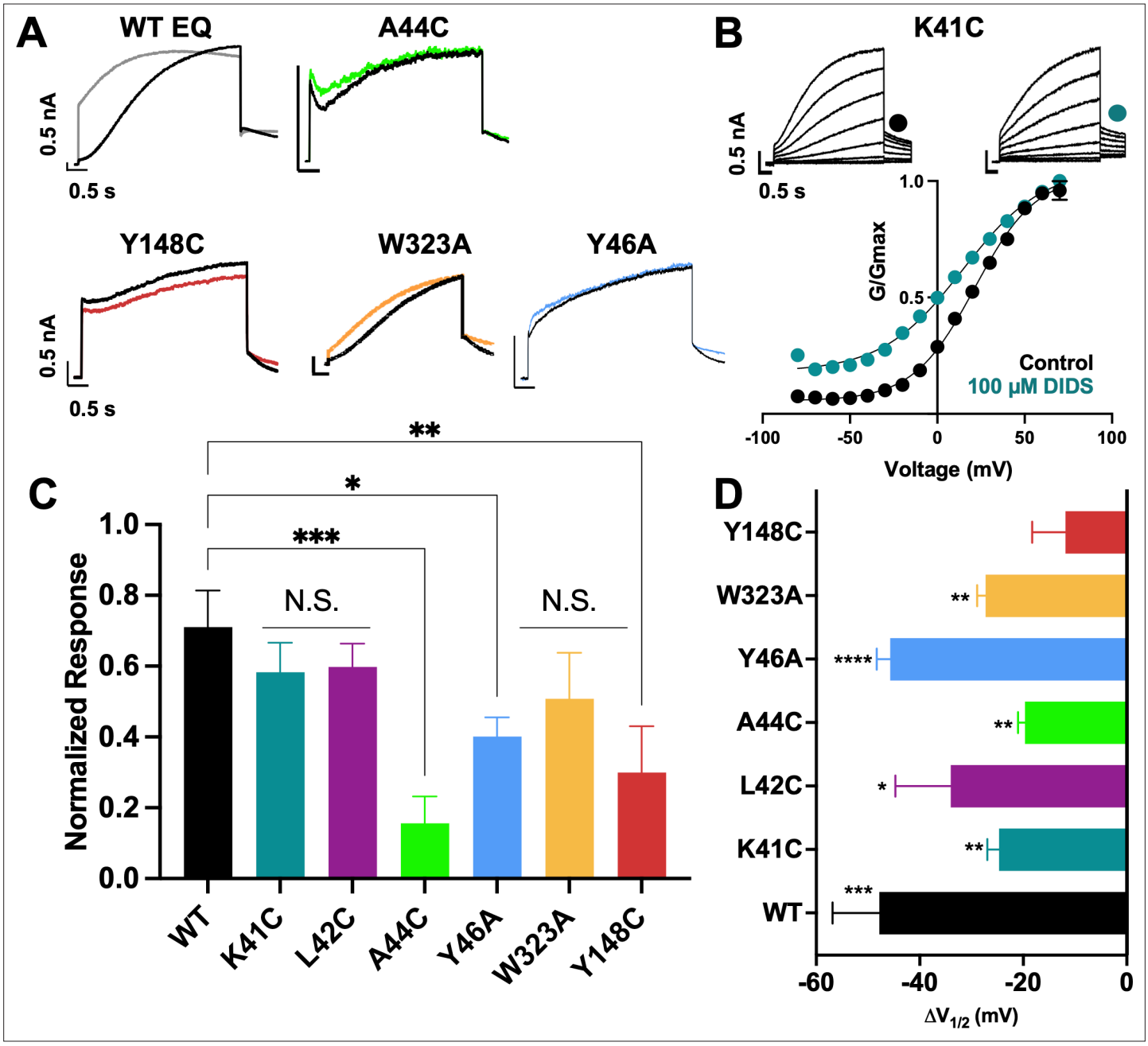

Figure 7. Binding site mutants important for the action of DIDS. (**A**) Current traces from WT EQ and key mutants in the absence (control; black) and presence (colors) of 100 µM DIDS. (**B**) Data and G-V plots in control (black) and DIDS (teal). Boltzmann fits were: K41C-EQ control (n=3): $V_{1/2}$ = 23.1 mV, *k*=20.2 mV; K41C-EQ DIDS (n=5): $V_{1/2}$ = -1.6 mV, *k*=24.0 mV. Voltage steps from a holding potential of –80 mV to +70 mV for 4 s, followed by repolarization to –40 mV for 1 s. Interpulse interval was 15 s. Error bars shown are ± SEM. All calibration bars denote 0.5 nA/0.5 s. (**C**) Summary plot of the normalized response to 100 µM DIDS. Data are shown as mean + SEM and *p<0.05, **p<0.01, ***P<0.001 denote significant change in mutant versus WT currents (one-way ANOVA, see Materials and methods). For calculation, see Materials and methods. (**D**) Change in $V_{1/2}$ ($\Delta V_{1/2}$) for WT EQ and each I_{Ks} mutant in control versus DIDS. Data are shown as mean - SEM and unpaired t-test was used, where *p<0.05, **p<0.01, ***p<0.001, ****p<0.0001 indicate a significant change in $V_{1/2}$ comparing control to the presence of drug. n-values for mutants in C and D are stated in ***Table 5***.

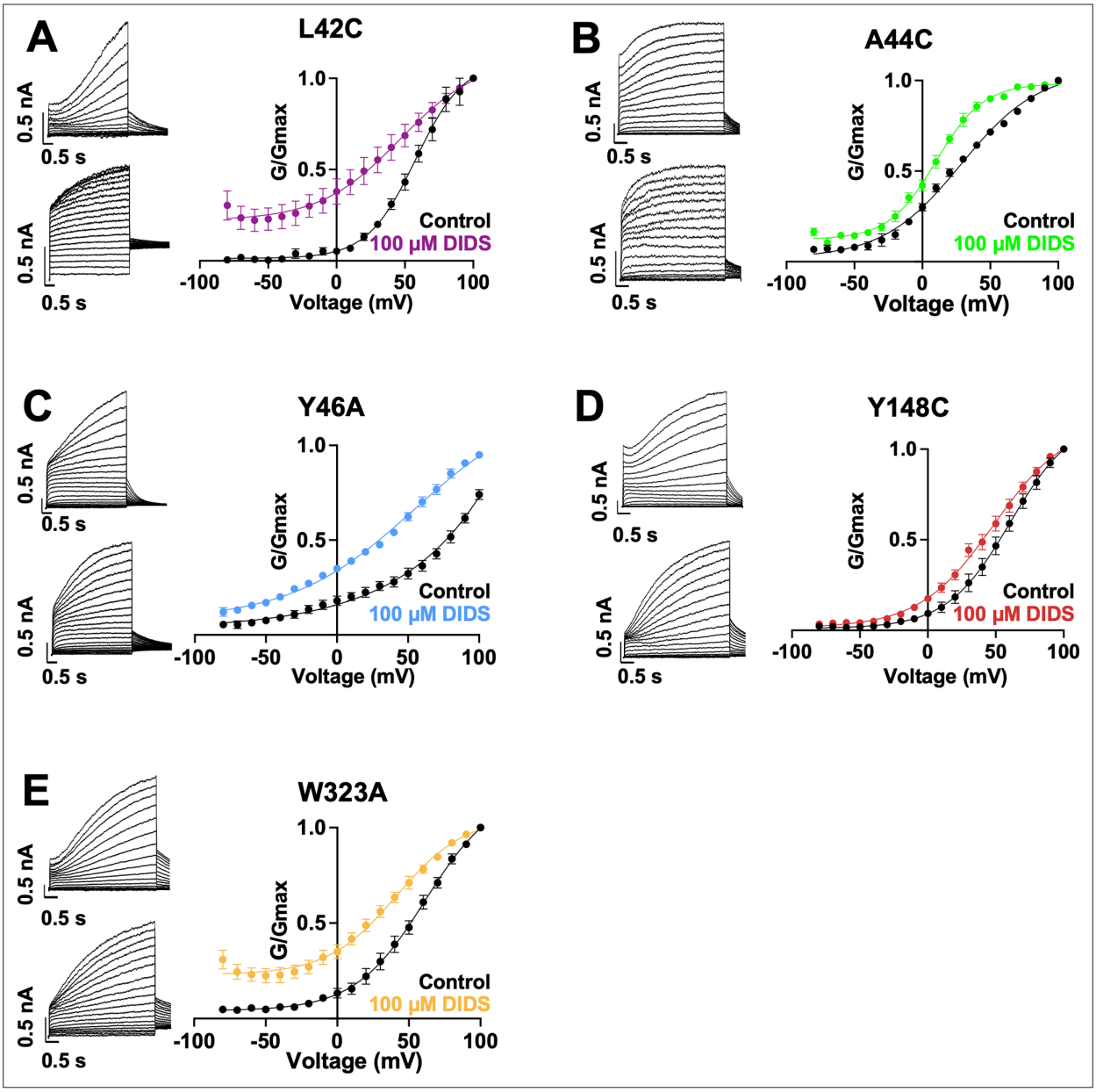

Figure 7—figure supplement 1. Current waveform and G-V changes induced by DIDS for all binding site mutants. (**A-E**) current traces in control (top) and presence of 100 μM DIDS (bottom). For binding site mutants, cells were held at –80 mV, then pulsed to between –90 mV and +100 mV for 4 s followed by –40 mV for 2 s. G-V plots in control (black) and presence of 100 μM Mef (colors). Error bars are ± SEM. Refer to ***Table 5*** for Boltzmann fit values.

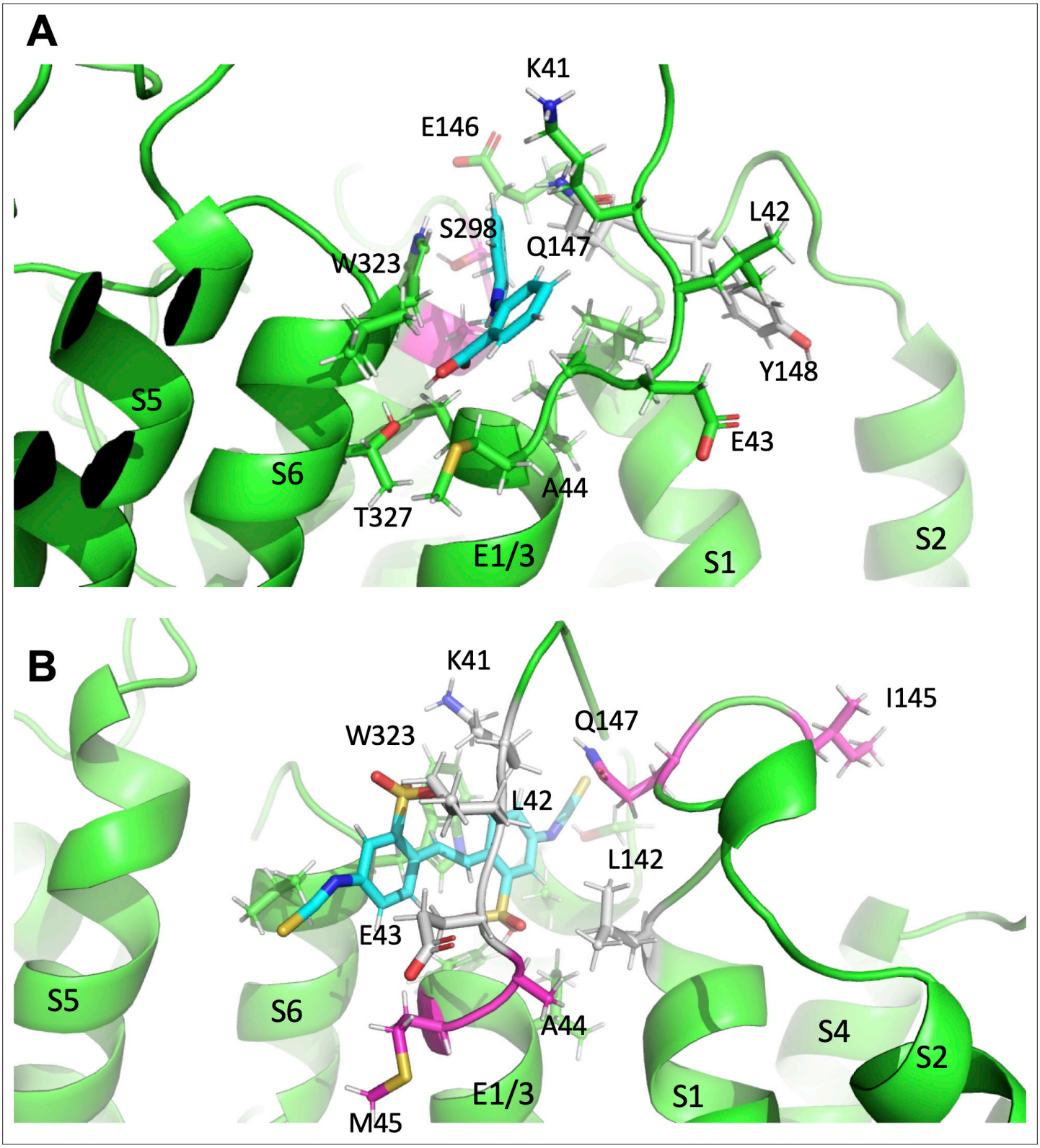

Figure 8. Subtle differences in activator binding to Y46C- and A44C-ps-I_{Ks} mutant channels. (**A**) Mefenamic acid bound to the ps-I_{Ks} channel. Residues that are part of the binding site are shown in stick format colored green, except those residues that were important in the WT channel that had reduced ΔG in Y46C (in grey). Residues that had slight increases in ΔG values in Y46C are shown in magenta (S298, A300). Mefenamic acid is in cyan. See ***Figure 8—source data 1***. (**B**) DIDS bound to the ps-I_{Ks} channel. Residues that are part of the binding site are shown in stick format colored green except those residues that were important in the WT channel that had reduced ΔG in the A44C mutant (in grey). Residues that had slight increases in ΔG values in

Figure 8 continued on next page

Figure 8 continued

A44C are shown in magenta. DIDS is in cyan. W323 may be seen behind DIDS. See ***Figure 8—source data 2***. Images were made with the PyMOL Molecular Graphics System, Version 2.0 Schrödinger, LLC.